Fabrication of Embedded 45-Degree Micromirror Using Liquid-Immersion Exposure for Single-Mode Optical Waveguides

Junichi Inoue, Tomonori Ogura, Kenji Kintaka, *Member, IEEE, OSA*, Kenzo Nishio, Yasuhiro Awatsuji, *Member, IEEE, OSA*, and Shogo Ura, *Member, IEEE, OSA*

***Abstract*—A new integration technique of a 45-degree micromirror providing a vertical coupling between a free-space wave and a guided wave in a dielectric-glass waveguide for high-density intra-board optical interconnection was described. A planar waveguide consisting of a 4-μm-thickness GeO_2:SiO_2 guiding core layer and a 2-μm-thickness SiO_2 cladding layer on an SiO_2 substrate was used for characterization of the micromirror. A trench with 8-μm depth and 8-μm width was formed in the waveguide by using a dry etching technique. A photoresist filling the trench was exposed at an angle of 45 degrees in the water to give a 45-degree taper in the trench. Au was evaporated on the taper to give high-reflection micromirror. An excess loss due to the micromirror insertion was estimated to be about 2 dB by comparing insertion losses of waveguides with and without the micromirror.**

***Index Terms*—Chip-to-chip optical interconnection, 45-degree micromirrors, liquid-immersion exposure technique, single-mode waveguides.**

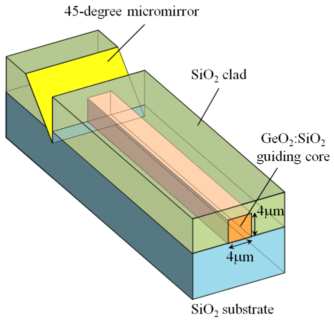

Fig. 1. Schematic perspective view of a waveguide with an embedded micromirror.

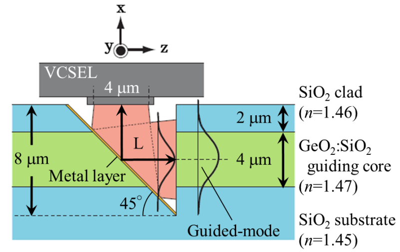

Fig. 2. Cross-sectional diagram of micromirror and input coupling of VCSEL to a waveguide.

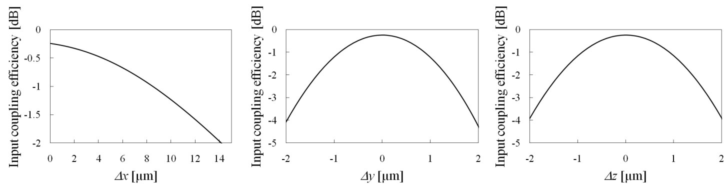

(a) (b) (c)

Fig. 3. Dependence of input coupling efficiency on VCSEL position gaps in x, y and z direction. (a) Dependence on Δx. (b) Dependence on Δy. (c) Dependence Δz on .

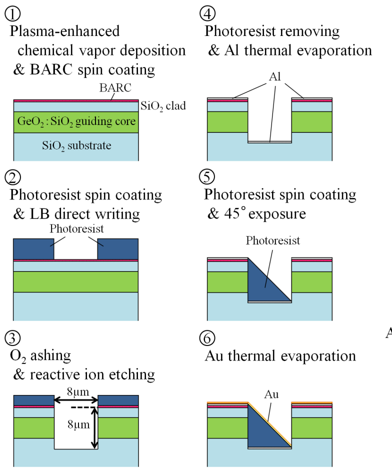

Fig. 4. Fabrication process of the micromirror.

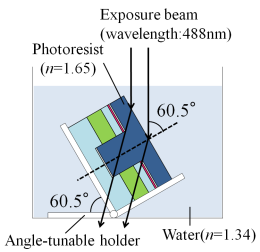

Fig. 5. Configuration of liquid immersion exposure.

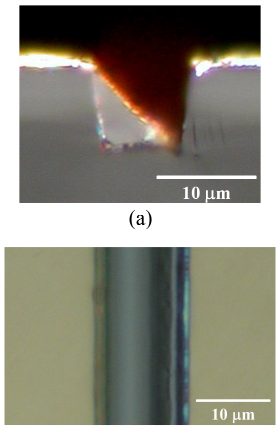

(a)

(b)

Fig. 6. Optical microscope photographs of cross-sectional (a) and top (b) views of the fabricated micromirror.

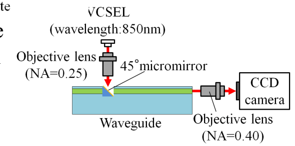

Fig. 7. Experimental setup for characterizing input coupling.

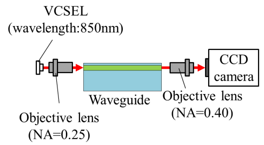

Fig. 9. Experimental setup for measuring insertion loss of the fabricated waveguide without micromirror.

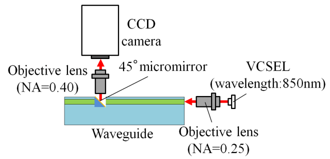

Fig. 11. Experimental setup for characterizing output coupling.

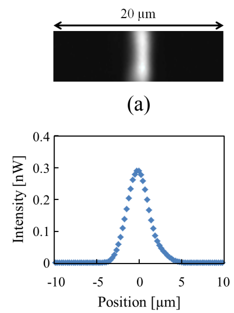

(a)

(b)

Fig. 8. Experimental result of input coupling. (a) Near-field image. (b) Intensity profile.

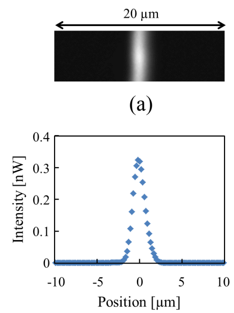

(a)

(b)

Fig. 10. Experimental result of fabricated waveguide without micromirror. (a) Near-field image. (b) Intensity profile.

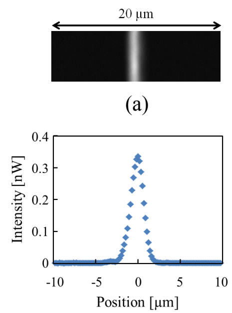

(a)

(b)

Fig. 12. Experimental result of output coupling. (a) Near-field image. (b) Intensity profile.